AD_____

Award Number: W81XWH-11-1-0371

TITLE: Intracellular Protein Delivery for Treating Breast Cancer

PRINCIPAL INVESTIGATOR: Dr. Yi Tang

CONTRACTING ORGANIZATION: University of Califronia, Los Angeles
Los Angeles, CA 90095

REPORT DATE: June 2012

TYPE OF REPORT: Annual

PREPARED FOR: U.S. Army Medical Research and Materiel Command
Fort Detrick, Maryland 21702-5012

DISTRIBUTION STATEMENT: Approved for public release; distribution unlimited

The views, opinions and/or findings contained in this report are those of the author(s) and should not be construed as an official Department of the Army position, policy or decision unless so designated by other documentation.

REPORT DOCUMENTATION PAGE

1. REPORT DATE (DD-MM-YYYY) 01-06-2012	2. REPORT TYPE Annual	3. DATES COVERED (From - To) 15 May 2011 - 14 May 2012

4. TITLE AND SUBTITLE	5a. CONTRACT NUMBER
Intracellular Protein Delivery for Treating Breast Cancer	5b. GRANT NUMBER W81XWH-11-1-0371
	5c. PROGRAM ELEMENT NUMBER

6. AUTHOR(S)	5d. PROJECT NUMBER
Dr. Yi Tang	5e. TASK NUMBER
E-Mail: yitang@ucla.edu	5f. WORK UNIT NUMBER

7. PERFORMING ORGANIZATION NAME(S) AND ADDRESS(ES)	8. PERFORMING ORGANIZATION REPORT NUMBER
University of California, Los Angeles Los Angeles, CA 90095	

9. SPONSORING / MONITORING AGENCY NAME(S) AND ADDRESS(ES)	10. SPONSOR/MONITOR'S ACRONYM(S)
U.S. Army Medical Research and Materiel Command Fort Detrick, Maryland 21702-5012	11. SPONSOR/MONITOR'S REPORT NUMBER(S)

12. DISTRIBUTION / AVAILABILITY STATEMENT
Approved for Public Release; Distribution Unlimited

13. SUPPLEMENTARY NOTES

14. ABSTRACT
The development of stimuli-responsive, nano-scale therapeutics that can selectively target tumors is a major research focus in cancer nanotechnology. A potent therapeutic option is directly arming the cancer cells with apoptotic-inducing proteins that are not targeted by anti-apoptotic maneuvers found in tumors. The avian virus derived apoptin forms a high molecular weight protein complex that selectively accumulates in the nuclei of cancer cells to induce apoptotic cell death. To enable the efficient delivery of this tumor-selective complex in functional form, we synthesized degradable, sub-100 nm, core-shell protein nanocapsules containing the 2.4 MDa apoptin complexes. Recombinant apoptin is reversibly encapsulated in a positively charged, water soluble polymeric shell and is released in native forms in response to reducing conditions such as the cytoplasm. The nanocapsules are efficiently internalized by mammalian cells lines as characterized by confocal microscopy, and rhodamine-labeled apoptin can be observed in the nuclei of cancer cells only. Released apoptin induced tumor-specific apoptosis in several cell lines and inhibited tumor growth in vivo, demonstrating the potential of this polymer-protein combination as a cancer therapeutic.

15. SUBJECT TERMS
Nanogels, core-shell, redox-responsive, apoptosis, breast cancer

16. SECURITY CLASSIFICATION OF:			17. LIMITATION OF ABSTRACT	18. NUMBER OF PAGES	19a. NAME OF RESPONSIBLE PERSON USAMRMC
a. REPORT U	b. ABSTRACT U	c. THIS PAGE U	UU	18	19b. TELEPHONE NUMBER (include area code)

Table of Contents

INTRODUCTION

Specific induction of cell death in tumors is considered one of the most desired and effective anticancer therapies. Effective strategies to activate the apoptotic pathway, or other death mechanisms, are currently being intensely pursued. A potent chemotherapy option is directly arming the cancer cells with executioner proteins or apoptotic-inducing proteins that are not targeted by anti-apoptotic maneuvers found in many tumors. In this proposal, we will develop a new method to treat breast cancer by using a native-protein delivery approach. This is a platform to deliver proteins in native forms into cells. The key design feature of our strategy is to first encapsulate protein molecules in a thin layer of water soluble, positively charged, degradable polymer to form nanometer-sized nanocapsules. The nanocapsule shell facilitates uptake of the protein content into cells, and protects the protein both during in vivo circulation and endocytosis. To endow the nanocapsules biodegradability once entered the target cells, the polymer shell is crosslinked with redox-sensitive crosslinkers that can be reduced upon encountering the reducing environment of the cytoplasm. Our overall research objective is to thoroughly evaluate this delivery method as a potentially new therapeutic modality for breast cancer treatment. Three aims will be pursued in parallel and results from each aim will be used to guide the refinement of other aims and the overall research objective. 1) Delivering different target proteins to breast cancer cell lines using this approach, including the tumor specific apoptin; 2) Equipping the protein nanocapsules with specific cancer cell targeting ligands; 3) Examining the in vivo potency and pharmacokinetics of the nanocapsules.

BODY

Summary of State of Work

Specific Aim 1: Delivering different target proteins to breast cancer cell lines using protein nanocapsules
Task 1. Preparing and characterizing of Apoptin contained nanocapsules
This task has been completed. Detailed description can be found in the following pages.

Task 2. *in vitro* studying Apoptin contained nanocapsules
This task has been completed. Detailed description can be found in the following pages.

Specific Aim 2: Equipping protein nanocapsules with specific cancer cell targeting ligands;
Task 3. Preparing and testing of MMP activatable cell penetrating peptides (ACCPs)-coupled nanocapsules
This task is currently under evaluation, no results to report at this point.

Task 4. Preparing and testing of ligand-receptor affinity based targeting: Transferrin (Tf) and Herceptin
This task is currently under evaluation, no results to report at this point.

Specific Aim 3: Examining the *in vivo* potency and pharmacokinetics of the nanocapsules.

Task 5. Evaluating *in vivo* distribution of protein nanocapsules
This task has been partially performed and some results will be in the following pages.

Task 6. Examining the *in vivo* pharmacokinetics of nanocapsules
This task is currently under evaluation, no results to report at this point.

Task 7. Determing the *in vivo* delivery efficacy of nanocapsules
This task has been completed. Detailed description can be found in the following pages.

The following results have been submitted for publication and has been reformatted here. Supplement referred to in the text can be found in APPENDIX.

1. BACKGROUND AND MOTIVATION

The most desirable cancer therapy is both potent and specific towards tumor cells [1,2]. Many conventional small molecule chemotheraputics do not discriminate between cancerous and normal cells, cause undesirable damage to healthy tissues, and are therefore unable to be administered at high dosage. In contrast, cytoplasmic and nuclear proteins that selectively alter the signaling pathways in tumor cells, reactivate apoptosis and restore tissue homeostasis, can eliminate cancerous cells and delay tumor progression with less collateral damage to other tissues [3-6]. Using stimuli-responsive nanoscaled carriers for the intracellular delivery of such proteins, including human tumor suppressors (such as p53 [7]) and exogenous tumor-killing proteins [8] (such as apoptin [9,10]), is attractive as a new anti-cancer therapy modality.

Apoptin is a 121-residue protein derived from chicken anemia virus [9]. When transgenically expressed, apoptin was shown to induce p53-independent apoptosis in a variety of tumor and transformed cells [11,12], while leaving normal and untransformed cells unaffected [13]. Apoptin exists in a globular multimer complex of thirty to forty subunits with no well-defined secondary structure [14]. While the exact mechanism of the tumor selectivity is unresolved, apoptin is known to translocate to the nuclei where tumor-specific phosphorylation at residue Thr108 takes place, leading to accumulation of apoptin in nuclei and activation of the apoptotic cascade in tumor cells [15]. In normal cells, apoptin is not phosphorylated at Thr108 and is located mostly in the cytoplasm, where it becomes aggregated and degraded [16]. Because of the high potency in inducing this exquisite tumor-selective apoptosis, apoptin has been investigated widely as an anti-tumor therapeutic option [9]. Different gene therapy approaches have been used to administer apoptin to mouse xenograft tumor models, in which significant reduction in tumor sizes and prolonged lifespan of mice have been observed without compromising the overall health [17-19]. However, as with other gain-of-function therapy candidates, *in vivo* gene delivery approaches, such as the use of viral vectors may lead to genetic modifications and elicit safety concerns [20]. Development of nanoparticle carriers to aid the functional delivery of apoptin to tumor cells is therefore desirable [21].

We chose to work with maltose-binding-protein fused apoptin (MBP-APO) which can be highly expressed in soluble form from *Escherichia coli*, whereas native apoptin form inclusion bodies [14]. MBP-APO has been shown by gel filtration to similarly assemble into a multimeric complex and to capture the essential functions and selectivity of native apoptin [14]. Nanoparticle-mediated delivery of functional MBP-APO poses unique challenges [22]. First, the protein cargo preassembles into large complexes with an average diameter of ~40 nm and molecular weight of ~2.4 MDa [14]. To achieve nanoscale sizes that are optimal for *in vivo* administration (~100 nm) [23], a loading strategy that leads to compact particles is preferred. Second, in order to maintain the noncovalent multimeric state of functional MBP-APO, the protein loading and releasing events need to take place under very mild, physiological conditions in the absence of surfactants. Lastly, the protein cargo must be released into the cytoplasm in its native functional form, including the correct spatial presentation of nuclear localization/export signals, as well as the phosphorylation site and downstream signalling elements within apoptin.

In the current study, we selected a polymeric nanocapsule strategy for the functional delivery of MBP-APO, in which the protein complex is nearly individually and noncovalently protected in a water soluble polymer shell (Figure 1). This slightly positively-charged shell protects the MBP-APO from serum proteases and harsh environment, as well as enables cellular uptake through endocytosis [24]. The polymeric layer is weaved together by redox-responsive cross-linkers containing disulfide bond (S-S), which can be degraded once the nanocapsules are exposed to the reducing environment in cytoplasm [25]. The noncovalent nature of the polymer shell ensures completely reversible encapsulation and release of native protein in the cell. Using this apporach, we showed that MBP-APO can be efficiently delivereid to different cell lines, and the fucntionality and selectivty of the administered apoptin towards cancer cell lines is demonstrated.

2. MATERIALS AND METHODS
2.1. Materials

N-(3-aminopropyl) methacrylamide hydrochloride was purchased from Polymer Science, Inc. CellTiter 96® AQueous One Solution Cell Proliferation Assay (MTS) reagent was purchased from Promega Corporation. APO-BrdU[TM] TUNEL Assay Kit was purchased from Invitrogen. *In situ* Cell Death Detection Kit, POD; was purchased from Roche Applied Science. Female athymic nude (*nu/nu*) mice, 6 weeks of age, were purchased from Charles River Laboratories (Wilmington, MA). All other chemicals were purchased from Sigma-Aldrich and used as received.

2.2. Protein nanocapsule preparation

The concentration of protein was diluted to 1 mg/mL with 5 mM sodium bicarbonate buffer at pH 9. Then 200 mg/mL acrylamide (AAm) monomer was added to 1 mL of protein solution with stirring at 4°C. After 10 min, the second monomer, *N*-(3-aminopropyl) methacrylamide (APMAAm), was added while stirring. Different cross-linkers, *N,N'*-methylene bisacrylamide for ND NC and *N,N'*-bis(acryloyl)cystamine for S-S NC, was added 5 min after the addition of APMAAm. The polymerization reaction was immediately initiated by adding 30 μL of ammonium persulfate (100 mg/mL, dissolved in deoxygenated and deionized water) and 3 μL of *N,N,N',N'*-tetramethylethylenediamine. The polymerization reaction was allowed to proceed for 60 min. The molar ratios of AAm/APMAAm/cross-linker used were 1.5:1:0.14, 2:1:0.14, 4:1:0.14, and 8:1:0.14. Buffer exchange with phosphate-buffered saline (PBS) buffer (pH 7.4) was used to remove the remaining monomers and initiators. Rhodamine-labeled APO NCs was obtained through encapsulation of MBP-APO modified with 5-Carboxy-X-rhodamine *N*-succinimidyl ester (mass ratio (MBP-APO: rhodamine): 4:1).
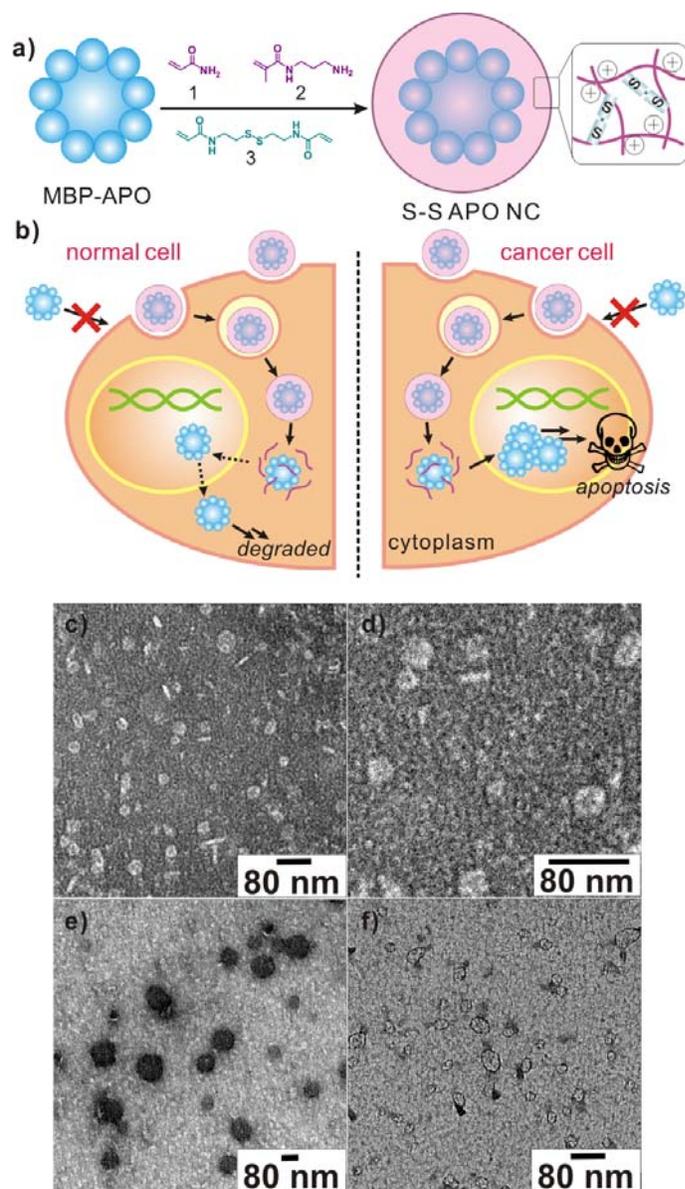

Figure 1. Degradable nanocapsules for apoptin delivery. a-b) Schematic diagram of synthesis of degradable apoptin nanocapsules (S-S APO NC) and delivery into tumor cells to induce apoptosis; TEM images of c) native MBP-APO; d) enlarged image of MBP-APO; e) S-S APO NC; and f) degraded S-S APO NC after treatment with 2 mM GSH for 6 hours at 37°C;

2.3. Characterization of protein nanocapsules.

The mean hydrodynamic size and ζ-potential of NC were determined by DLS in PBS buffer. Samples of NCs (0.05 mg/mL) for TEM imaging were negatively stained with 2 % uranyl acetate in alcoholic solution (50 % ethanol). The lamella of stained sample was prepared on carbon-coated electron microscopy grids (Ted Pella, Inc.).

2.4. Cellular uptake and localization of nanocapsules

MDA-MB-231, HeLa, MCF-7, and human foreskin fibroblast (HFF) cells (ATCC, Manassas, VA) were cultured in Dulbecco's Modified Eagle's Media (DMEM) (Invitrogen) supplemented with 10% bovine growth serum (Hyclone, Logan, UT), 1.5 g/L sodium bicarbonate, 100 μg/mL streptomycin and 100 U/mL penicillin, at 37 °C with 98% humidity and 5% CO$_2$. To visualize NCs uptake, MDA-MB-231 cells were seeded into 48-

well plate, with a density of 10,000 cells/well in 250 µL of media with supplements. S-S Rho-APO NC and ND Rho-APO NC were added to a final concentration of 20 nM. After 1 hour and 24 hours of incubation, cells were washed with PBS twice, stained with DAPI Nucleic Acid Stain and imaged. For internalization of S-S Rho-APO NC with different ζ-potentials, MDA-MB-231 cells were incubated with 20 nM NCs for 2 hours before nuclei staining. Markers for early and late endosomes were used for internalization trafficking study. A concentration of 20 nM S-S Rho-APO NCs was added to HeLa cells and incubated for 30 min, 60 min and 120 min under 37 °C. Cells were then fixed with 4 % formaldehyde, permeabilized with 0.1 % Triton X-100, and stained with antibodies, mouse anti-EEA1 antibody against early endosomes and rabbit anti-CI-MPR antibody against late endosomes (Cell Signaling Technology, Inc.). Texas red goat anti-mouse IgG and Alexa Fluor® 647 goat anti-rabbit IgG (Invitrogen) were added as the secondary antibody. To determine the cellular localization of the protein delivered, confocal images were taken with HeLa, MCF-7, and HFF cells incubated with 20nM of S-S Rho-APO NC or ND Rho-APO NC at 37°C for 24 hours. Nuclei were then counterstained with DAPI. The Z stack images of cells were imaged at 0.4-µm intervals and analyzed by Nikon NIS Element software. Fluorescent images were acquired on a Yokogawa spinning-disk confocal scanner system (Solamere Technology Group, Salt Lake City, UT) using a Nikon eclipse Ti-E microscope equipped with a 60×/1.49 Apo TIRF oil objective and a Cascade II: 512 EMCCD camera (Photometrics, Tucson, AZ, USA). An AOTF (acousto-optical tunable filter) controlled laser-merge system (Solamere Technology Group Inc.) was used to provide illumination power at each of the following laser lines: 491 nm, 561nm, and 640 nm solid state lasers (50mW for each laser).

2.5. Cytotoxicty Assays

Different cancer cells lines, HeLa, MCF-7 and MDA-MB-231, as well as noncancerous HFF, were seeded into 96-well plates, each well containing 5,000 cells in 100 µL of DMEM with supplements. Different concentrations of protein and NCs were added into each well and the plates. After incubation of 48 hours at 37°C, the wells were washed with PBS solution twice and 100 µL of fresh cell culture media with supplements was added. Then 20 µL MTS solution (CellTiter 96® AQueous One Solution Cell Proliferation Assay) was added into each well and the plates were incubated for 3 hours at 37 °C. The absorbance of product was read at 490 nm using a microplate reader (PowerWave X, Bio-tek Instruments, USA). Apoptosis of cells was detected using APO-BrdU Terminal Deoxynucleotidyl Transferase dUTP Nick End Labeling (TUNEL) assay kit. MDA-MB-231 and HFF cells were seeded at a density of 100,000 cells/well into a 6-well plate in 2 mL of cell culture media with supplements. Proteins and NCs were added after cells covered 80% of bottom surface. After 24 hours of incubation, cells were fixed with 1% paraformaldehyde in PBS, followed by the addition of DNA labeling solution containing terminal deoxynucleotidyl transferase and bromodeoxyuridine (BrdUrd). Cells were then stained with Alexa Fluor® 488 dye-labeled anti-BrdUrd antibody. Samples were deposited onto slides, which were later stained with propidium iodide (PI) solution containing RNase A. Images were obtained by fluorescence microscope (Zeiss, Observer Z1) using appropriate filters for Alexa Fluor 488 and PI.

2.6. *In vivo* studies with MCF-7 xenograft model

All mice were housed in an animal facility at the University of Southern California in accordance with institute regulations. Female athymic nude (*nu/nu*) mice were subcutaneously grafted on the back flank with $5×10^6$ MCF-7 tumor cells. Afterwards, tumor size was monitored by a fine caliper and the tumor volume was calculated as the product of the two largest perpendicular diameters and the vertical thickness (L×W×D, mm^3). When the tumor volume reached 100-200 mm^3, mice were randomly separated into different groups. From day 0, mice were treated with intratumoral injection of native MBP-APO or S-S APO NC (200µg per mouse) every other day. PBS and S-S BSA NC were included as the negative controls. When the tumor volume oversized 2500mm^3, the mice were euthanized by CO_2 according animal protocol. The average of tumor volume was plotted as the tumor growth curve in respective treated groups. For histology study, treated tumor samples were collected and fixed in 4% paraformaldehyde, and processed for staining using the *In Situ* Cell Death Detection Kit. The stained tumor slides were observed under microscope, and representative pictures were taken for analysis. Paraformaldehyde-postfixed frozen tumor sections (5-µm thick) were permeabilized with 0.1% triton X-100 and stained with TUNEL assay kit (In Situ Cell Death Detection Kit, POD; Roche Applied Science,

Indianapolis, IN) in accordance with the manufacturer's instructions. DAPI was used for nuclear counterstaining.

3. RESULTS AND DISCUSSION

3.1. Synthesis and characterization of apoptin nanocapsules

MBP-APO (pI = 6.5) was first purified from *E. coli* extract using an amylose-affinity column (Supplement 2 and Supplement 8). Dynamic Light Scattering (DLS) measurement revealed an average hydrodynamic radius of 36.1 nm (Supplement 3), consistent with the reported size for the MBP-APO complex [14]. Transmission Electron Microscopy (TEM) analysis of MBP-APO showed similarly sized protein complexes (Figure 1c and enlarged in Figure 1d). Interestingly, MBP-APO complexes appear to adopt a disk-shaped structure despite the lack of defined secondary structure from the apoptin component. Since the apoptin portion of the protein can self-assemble into the ~40-mer complex, we propose a three dimensional arrangement of MBP-APO in which the C-terminal apoptin forms the central spoke of the wheel-like structure (Figure 1b), with the larger MBP portion distributed around on the edge. The planar arrangement allows the apoptin portion of the fusion protein to remain accessible to its protein partners, which may explain how the MBP-APO fusion retains essentially all of the observed functions of native apoptin.

The reversible encapsulation strategy for producing apoptin nanocapsules (NCs) is shown in Figure 1a. Following electrostatic deposition of the monomers acrylamide (**1** in Figure 1a) and *N*-(3-aminopropyl)methacrylamide (**2**), and the cross-linker *N,N'*-bis(acryloyl)cystamine (**3**), at a molar ratio of 1.5:1:0.14, onto MBP-APO (1 mg) in carbonate buffer (5 mM, pH 9.0), *in situ* polymerization was initiated with the addition of free radical initiators and proceeded for one hour. The molar ratio and the time of reaction reported are optimized to minimize protein aggregation and precipitation, as well as to maximize the solution stability of the nanocapsule formed (S-S APO NC). Excess monomers and cross-linkers were removed using ultrafiltration and the S-S APO NC was stored in PBS buffer (pH 7.4). DLS clearly showed increase in average diameter of the sample to ~75 nm with a slightly positive ζ-potential value of 2.8 mV (Supplement 1). TEM analysis of the S-S APO NC confirmed the nearly doubling in diameter of the spherical particle (Figure 1e). Unexpectedly, the NCs displayed dark contrast upon uranyl acetate staining, which hints that the cores of the particles are very densely packed. As expected from the redox-responsive cross-linkers **3**, the reduction of NCs size can be seen upon treatment of the reducing agent glutathione (GSH) (2 mM, 6 hours, 37°C). As shown in Figure 1f, the densely packed NCs were completely dissociated into ~30 nm particles, confirming the reversible nature of the encapsulation process. As a control, we also synthesized nondegradable apoptin NCs (ND APO NC) using *N,N'*-methylene bisacrylamide as the cross-linker with same reagents concentrations under identical reaction conditions. Whereas similarly sized NCs were formed, no degradation can be observed in the presence of GSH.

3.2. Cellular uptake and localization of nanocapsules

We next examined the cellular uptake of the S-S APO NC and cellular localization of the cargo. If the unique tumor selectivity of MBP-APO is maintained following the encapsulation and release processes, we expect to find MBP-APO to enter the nucleus of the tumor cell, whereas in noncancerous cell it resides in the cytoplasm. Prior to the polymerization process, the MBP-APO protein was conjugated to amine-reactive rhodamine (Rho-APO) as described in 2.2. Subsequent encapsulation yielded similarly sized NCs as untagged APO NCs. Fluorescent images showed all NCs readily penetrated the cell membrane and were localized in the cytoplasm of MDA-MB-231 cells within one hour (Supplement 4). When decreasing the positively-charged monomer in the overall NC compostition, the NC surface became more neutral as determined by DLS and less cellular internalization were observed (Supplement 5). The cellular trafficking of the internalized S-S APO NCs in HeLa cells was also investigated for 2 hours by monitoring colocalization using markers for early and late endosomes (Figure 2a and Supplement 6). Highest levels of colocalization of Rho-APO and early endosome was detected at 30 minutes and decreased at later time points. In contrast, colocalization of Rho-APO and late endosome remained low throughout. Colocalization of nuclei stain and Rho-APO became evident at 2 hours, indicating endosomal escape and nuclear entry of the released apoptin protein. These results suggested that S-S APO NC were trafficked into early endosomes upon internalization and at least a significant portion of the internalized NCs and the cargo can escape from the endosomal compartment.

7

To analyze protein localization using confocal microscopy, two cancer cell lines HeLa and MCF-7, together with the noncancerous human foreskin fibroblast (HFF), were treated with either S-S Rho-APO NC or ND Rho-APO NC (Figure 2b). In the case of ND Rho-APO NCs, red fluorescence signals remained in the cytoplasm for all three cell lines, indicating the MBP-APO was well-shielded by the nondegradable polymer shell and its nuclear localization signals is not accessible to the transport machinery. In stark contrast, when HeLa cells were treated with S-S Rho-APO NC, strong red fluorescence of rhodamine was localized in the nuclei, resulting in intense pink color as a result of overlapping of rhodamine and DAPI fluorescence. Z-stacking analysis confirmed the MBP-APO to be localized inside of the nuclei. Similar results were observed with MCF-7 cells, although the fluorescence intensity was not as strong as in the HeLa cells. These results confirmed that the MBP-APO delivered can indeed be released in native forms inside the cytoplasm and enter the nuclei. More importantly, the specificity of MBO-APO delivered towards cancer cell lines were demonstrated in the confocal image of noncancerous HFF cells treated with S-S Rho-APO NC, as all of the dye signals remained in the cytoplasm and no nuclear accumulation can be observed.
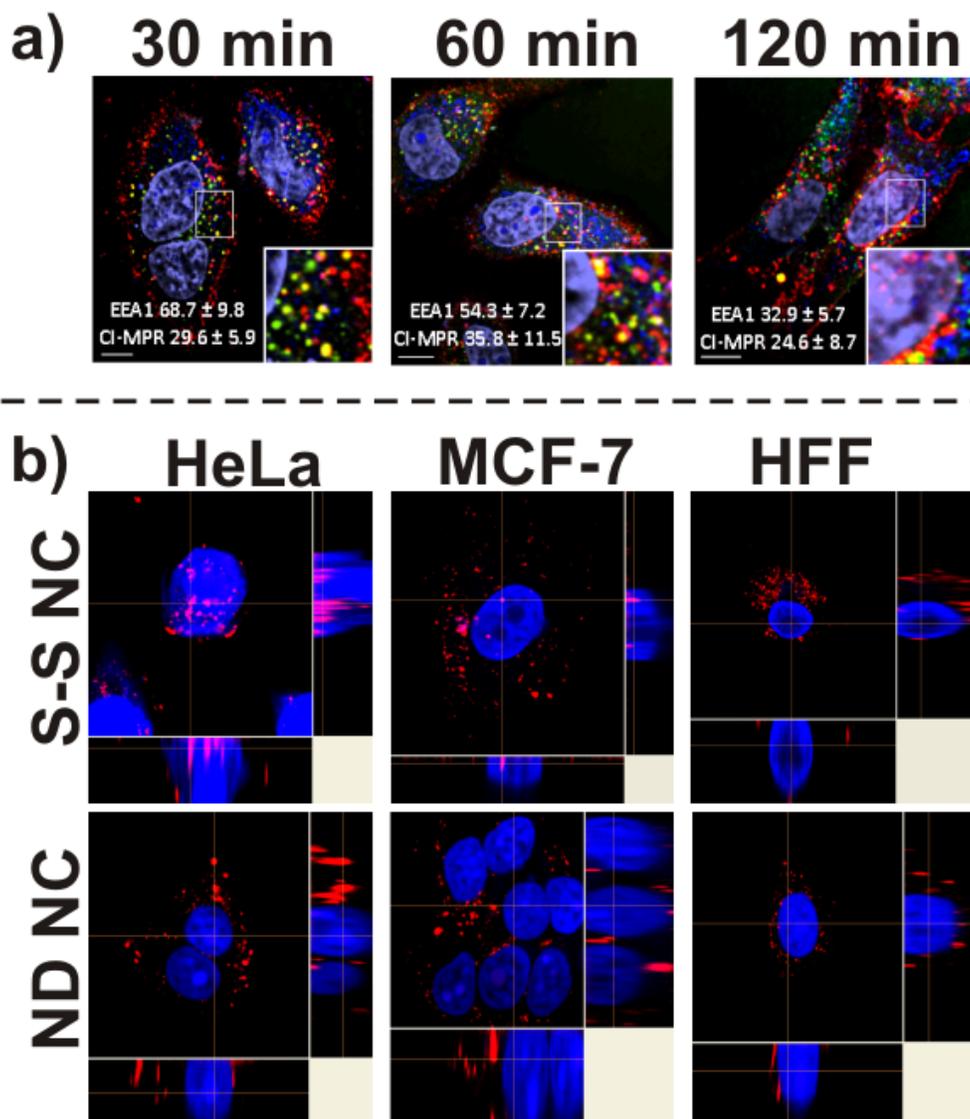

Figure 2. Protein nanocapsule cellular trafficking and localization. a) The trafficking of Rho-APO in S-S NCs through endosomes. HeLa cells were incubated with 20 nM S-S Rho-APO NCs (red) at 37 °C for various time periods, 30, 60 and 120 min. Early endosomes were detected by early endosome antigen 1 (EEA1, green). Late endosomes were detected by cation-independent mannose-6-phosphate receptor (CI-MPR, blue). Nuclei were stained with DAPI and shown as purple. The scale bar represents 10 μm. The percentage of fluorescence colocalization was quantified by calculating colocalization coefficients using Manders' overlap coefficient (>10 samples) and shown in each figure; b) confocal microscopy of cellular localization of Rho-APO encapsulated in S-S NC and ND NC to cancer cell lines HeLa and MCF-7, and noncancerous HFF. Nuclei were stained with DAPI (blue). The scale bar is 20 μm.

3.3. Tumor-selective cytotoxicity of apoptin nanocapsules

We then investigated whether the MBP-APO protein delivered still possess its function to induce tumor-selective apoptosis. The potency and selectivity of S-S APO NC were tested on various cell lines including HeLa, MCF-7, MDA-MB-231, and HFF (Figure 3a-d). MTS assay was used to measure cell viability 48 hours after addition of the protein and NC. For each cell line, ND APO NC and native MBP-APO were used as negative controls. When S-S APO NC was added to a final concentration of 200 nM, all three cancer cell lines had no viable cells, whereas ~75 % of the HFF had survived. The IC_{50} values were 80 and 30 nM for HeLa and MDA-MB-231, respectively. The IC_{50} for MCF-7 was higher at ~110 nM, which may be due to the deficiency in the terminal executioner caspase 3 and reliance on other effector caspases for apoptosis [26-27]. As expected, native MBP-APO and ND APO NC did not significantly decrease the viability of any cell lines tested, consistent with the inability to enter cells and release MBP-APO in cytoplasm, respectively. The IC_{50} values of S-S APO NC towards MDA-MB-231 increased as the surface charge of the NC became more neutral (Supplement 5), suggesting more efficient internalization can improve S-S NCs cytotoxicity. The morphologies of MDA-MB-231 and HFF cells were examined under various treatments. Only the S-S APO NC treated MDA-MB-231 cells exhibited blebbing and shrinkage, hallmarks of apoptotic cell death (Figure 3e and Supplement 7). Using TUNEL assay, S-S APO NC treated MDA-MB-231 also showed nuclear fragmentation associated with apoptosis, whereas all other samples, native MBP-APO and ND APO NC at the same concentration (Supplement 7), as well as HFF treated with 200 nM S-S APO NC (Figure 3e), had no sign of apoptosis. Collectively, these results demonstrated that the released MBP-APO upon degradation in cytoplasm retains the potency and selectivity as the transgenically expressed apoptin in previous studies [9].
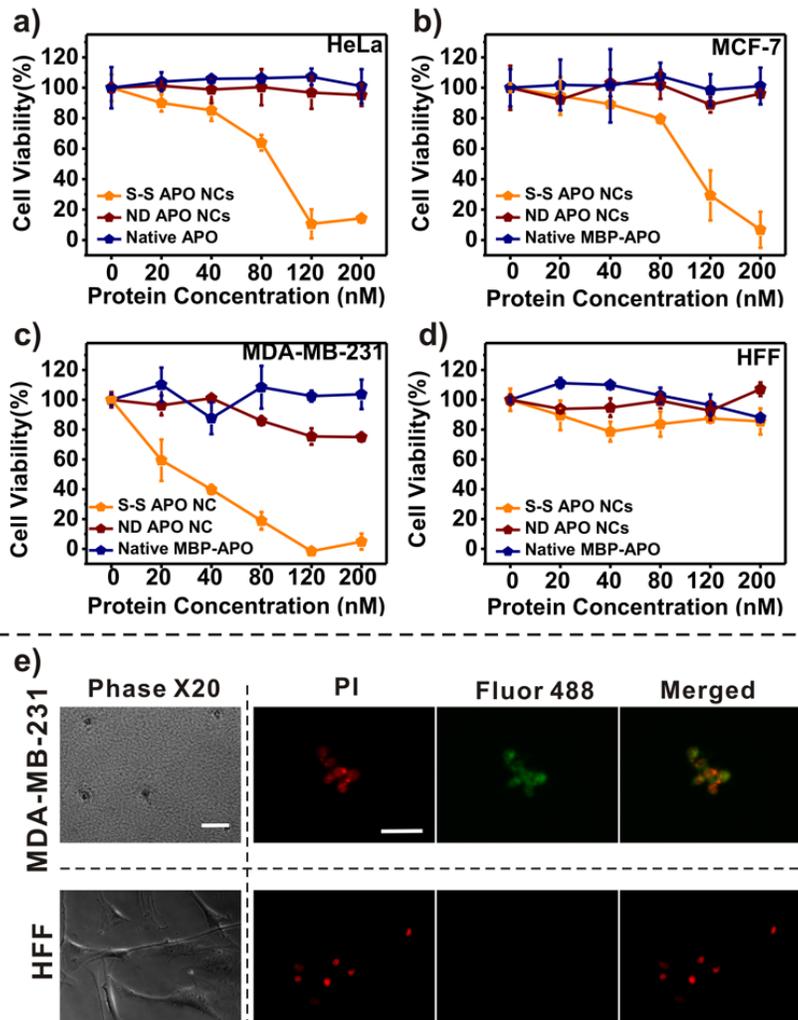

Figure 3. Cytotoxicity and apoptosis observed following nanocapsule delivery. (a) HeLa; (b) MCF-7; (c) MDA-MB-231; or (d) HFF cells with treatment of different concentrations of S-S APO NC, ND APO NC, and native MBP-APO. (e) Apoptosis induced by S-S APO NC determined by TUNEL assay. Images on the left are bright field microscopy images of MDA-MB-231 and HFF cells treated for 24 hours with 200 nM S-S APO NC. The scale bar represents 50 μm. Images right of the dash line shows detection of apoptotic fragmentation of the nucleosome after same treatment using APO-BrdU™ TUNEL assay kit. The scale bar represents 50 μm. Red fluorescence represents the propidium-iodide (PI)-stained total DNA, and green fluorescence represents the Alexa Fluor 488-stained nick end label, the indicator of apoptotic DNA fragmentation. The merged pictures combine the PI-stained nuclei and the Alexa Fluor 488-stained nick end label. (Note the bright field images do not overlap with the fluorescent images; cells were detached and collected for TUNEL assay after treatment).

3.4. In vivo evaluation of apoptin nanocapsules

We further examined the potency of S-S APO NC in mouse xenograft model. Female athymic nude (*nu/nu*) mice were subcutaneously grafted on the back flank with 5×10^6 MCF-7 breast cancer cells. When the tumor volume reached 100-200 mm^3 (day 0), mice were randomly separated into different groups and treated with intratumoral injection of PBS, MBP-APO, S-S APO NC. In addition, S-S NC with bovine serum albumin (S-S BSA NC) was added as a nonlethal protein cargo control testing the effects of the S-S NC polymer component on tumor cells *in vivo*. Tumors treated with saline, S-S BSA NC or native MBP-APO expanded rapidly and reached the maximum limit (>2500 mm^3) within 12 days. In sharp contrast, tumor growth was significantly delayed when treated with S-S APO NC (Figure 4a). Fixed tumor tissues collected from each treatment group was examined for DNA fragmentation using *in situ* TUNEL assay. The images revealed the highest level of cell apoptosis for the tumor harvested from mice treated with S-S APO NC, correlating well with the significantly delayed tumor growth observed for this treatment group and confirming that tumor growth inhibition was indeed due to apoptin-mediated apoptosis (Figure 4b). Collectively, the xenograft study verified that the degradable nanocapsule effectively delivered recombinant MBP-APO proteins to tumor cells *in vivo*, which was highly effective in limiting tumor progression.
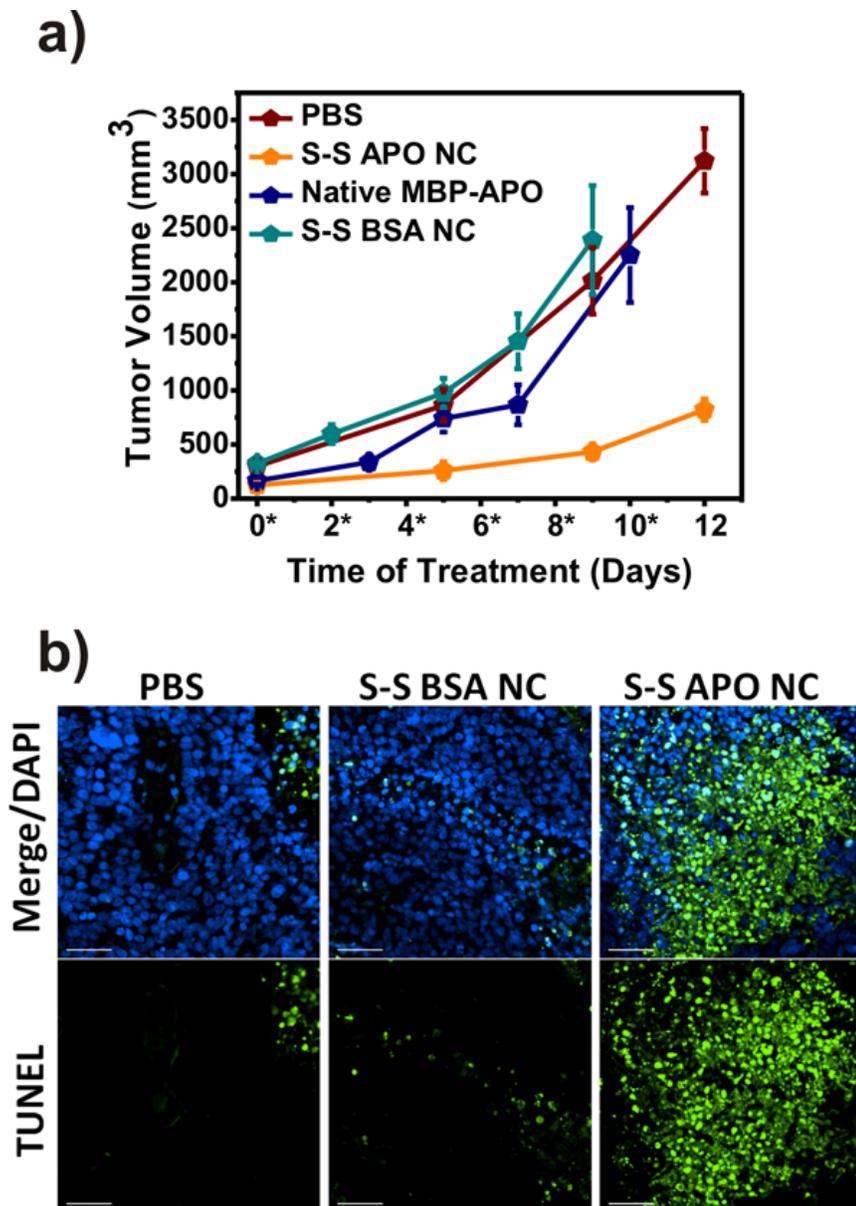

Figure 4. Treatment of apoptin nanocapsules resulted in tumor growth retardation. a) Significant tumor inhibition was observed in the mice treated by S-S APO NC. Female athymic nude mice were subcutaneously grafted with MCF-7 cells and treated with intratumoral injection of MBP-APO (n=4) or S-S APO NC (n=4) (200 µg/mouse) every other day. PBS (n=3) and S-S BSA NC (n=4) were included as negative controls. The average tumor volumes were plotted vs. time. Asterisks indicate injection days. b) Detection of apoptosis in tumor tissues after treatment with different NCs. Cross-sections of MCF-7 tumors were stained with fluorescein-dUTP (green) for apoptosis and DAPI for nucleus (blue). The scale bars represent 50 µm.

KEY RESEARCH ACCOMPLISHMENTS

- We synthesized polymer nanocapsules for delivery of tumor-selective protein complex derived from apoptin.

- The nanocapsule can be internalized by different tumor cells and the protein cargo is released intracellularly in response to the reducing environment of the cytoplasm.

- Released apoptin complex induced tumor-specific apoptosis in several cell lines and inhibited tumor growth *in vivo*.

REPORTABLE OUTCOMES

Publications*:*
The results above have been submitted for publication in *Nano Today*

Zhao, M., Hu, B., Gu, Z., Joo, K., Wang, P., Tang, Y. "Degradable Polymeric Nanocapsule for Efficient Intracellular Delivery of a High Molecular Weight Tumor-Selective Protein Complex." *Nano Today.* **2012**, *submitted*

Presentations:

The PI Tang has made the following presentations in which this material has been included.
NAE Indo-American Frontiers of Engineering Symposium, Crystal City, VA, March 2012
Department of Chemistry, California State University Long Beach, October 2011

The following poster presentation was made at the American Association for Cancer Research Special Conference: Molecular Targets and Cancer Therapeutics. November 12-16, 2011, San Francisco

"Delivery of tumor killing protein to cancer cells." Muxun Zhao, Biliang Hu, Pin Wang, Yi Tang. University of California, Los Angeles, Los Angeles, CA; University of Southern California, Los Angeles, CA

CONCLUSION

We were able to deliver the high molecular weight complex of the tumor-selective MBP-APO using a redox-responsive polymeric nanocapsule *in vitro* and *in vivo*. The choice and design of the sub-100 nm nanocapsule is well-suited for diverse protein targets because of its mild preparation conditions, completely reversible encapsulation and efficient cell membrane penetration/release of the protein cargo in the cytoplasm. Our application here further illustrates how intracellular protein delivery using nanoscale system can provide new possibilities for achieving selective cancer therapy.
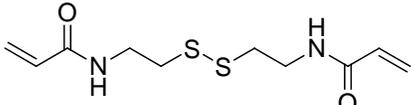
REFERENCES

[1]   J. B. Gibbs, Science, 287 (2000) 1969.
[2]   J. H. Atkins, L. J. Gershell, Nat. Rev. Drug. Discov. 1(2002) 491.
[3]   G. I. Evans, K. H. Vousden, Nature 411 (2001) 342.
[4]   J. C. Reed, Cancer Cell 3 (2003) 17.
[5]   T. G. Cotter, Nat. Rev. Cancer 9 (2009) 501.
[6]   A. Russo, M. Terrasi, V. Agnese, D. Santini, V. Bazan, Ann. Oncol. 17 (2006) 115.

[7]   C. J. Brown, S. Lain, C. S. Verma, A. R. Fersht, D. P. Lane, Nat. Rev. Cancer, 2009, 9, 862.

[8]   M. H. M. Noteborn, Euro. J. Pharmacol. 625 (2009) 165.

[9]   C. Backendorf, A. E. Visser, A. G. de Boer, R. Zimmerman, M. Visser, P. Voskamp, Y. H. Zhang, M. Noteborn, Annu. Rev. Pharmacol. Toxicol. 48 (2008) 143.

[10]   M. Los, S. Panigrahi, I. Rashedi, S. Mandal, J. Stetefeld, F. Essmann, K. Schulze-Osthoff, Biochim. Biophys. Acta. 1793 (2009) 1335.

[11]   S. M. Zhuang, A. Shvarts, H. van Ormondt, A. G. Jochemsen, A. J. van der Eb, M. H. Noteborn, Cancer Res. 55 (1995) 486.

[12]   J. G. Teodoro, D. W. Heilman, A. E. Parker, M. R. Green, Genes Dev. 18 (2004) 1952.

[13]   A. A. A. M. Danen-Van Oorschot, D. F. Fischer, J. M. Grimbergen, B. Klein, S. M. Zhuang, J. H. F. Falkenburg, C. Backendorf, P. H. A. Quax, A. J. Van der Eb, M. H. M. Noteborn, Proc. Natl. Acad. Sci. USA 94 (1997) 5843.

[14]   S. R. Leliveld, Y. H. Zhang, J. L. Rohn, M. H. Noteborn, J. P. Abrahams, J Biol. Chem. 278 (2003) 9042.

[15]   A. A. A. M. Danen-Van Oorschot, Y. H. Zhang, S. R. Leviveld, J. L. Rohn, M. C. M. J. Seelen, M. W. Bolk, A. van Zon., S. J. Erkeland, J. P. Abrahams, D. Mumberg, M. H. M. Noteborn, J. Biol. Chem., 278 (2003) 27729.

[16]   J. L. Rohn, Y. H. Zhang, R. I. Aalbers, N. Otto, J. Den Hertog, N. V. Henriquez, C. J. Van De Velde, P. J. Kuppen, D. Mumberg, P. Donner, M. H. Noteborn, J. Biol. Chem. 277 (2002) 50820.

[17]   A. M. Pietersen, M. M. van der Eb, H. J. Rademaker, D. J. van den Wollenberg, M. J. Rabelink, P. J. Kuppen, J. H. van Dierendonck, H. van Ormondt, D. Masman, C. J. van de Velde, A. J. van der Eb, R. C. Hoeben, M. H. Noteborn, Gene Ther. 6 (1999) 882.

[18]   M. M. van der Eb, A. M. Pietersen, F. M. Speetjens, P. J. Kuppen, C. J. van de Velde, M. H. Noteborn, R. C. Hoeben, Cancer Gene Ther. 9 (2002) 53.

[19]   D. J. Peng, J. Sun, Y. Z. Wang, J. Tian, Y. H. Zhang, M. H. Noteborn, S. Qu, Cancer Gene. Ther. 14 (2007) 66.

[20]   M. L. Edelstein, M. R. Abedi, J. Wixon, J. Gene. Med. 9 (2007) 833.

[21]   J. Shi, A. R. Votruba, O. C. Farokhzad, R. Langer, Nano Lett. 10 (2010) 3223.

[22]   Z. Gu, A. Biswas, M. Zhao, Y. Tang, Chem. Soc. Rev. 40 (2011) 3638.

[23]   P. P. Adiseshaiah, J. B. Hall, S. E. McNeil, Nanomed. Nanobi. 2 (2010) 99.

[24]   Z. Gu , M. Yan, B. Hu, K. I. Joo, A. Biswas, Y. Huang, Y. Lu, P. Wang, Y. Tang, Nano Lett. 9 (2009) 4533.

[25]   M. Zhao, A. Biswas, B. L. Hu, K. I. Joo, P. Wang, Z. Gu, Y. Tang, Biomaterials 32 (2011) 5223.

[26]   M. Burek, S. Maddika, C. J. Burek, P. T. Daniel, K. Schulze-Osthoff, M. Los, Oncogene 25 (2006) 2213.

[27]   R. U. Janicke, M. L. Sprengart, M. R. Wati, A. G. Porter, J. Biol. Chem., 273 (1998) 9357.

APPENDICES

Supplement Figures and Tables Presented in BODY.

**Supplement 1.** Mean hydrodynamic size and ζ- potential of protein NC

|	S-S APO NC	S-S BSA NC	ND APO NC
Size (nm)	74.71	10	79.58
ζ-poteintial (mV)	2.8±0.2	4.7±0.4	1.6±0.4
Crosslinker	*N,N'*-bis(acryloyl)cystamine		*N,N'*-methylene bisacrylamide
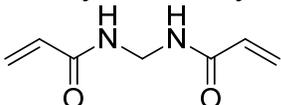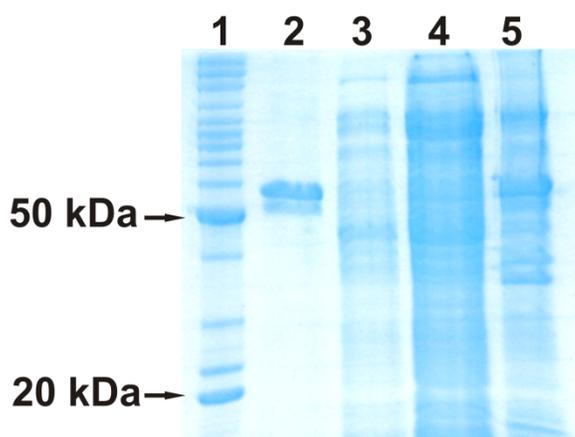
Supplement 2. SDS-PAGE for denatured MBP-APO samples. Lane 1 Molecular weight marker; Lane 2 Purified MBP-APO; Lane 3 Wash fraction; Lane 4 Unbounded cell lysate proteins; Lane 5 Insoluble fractions.
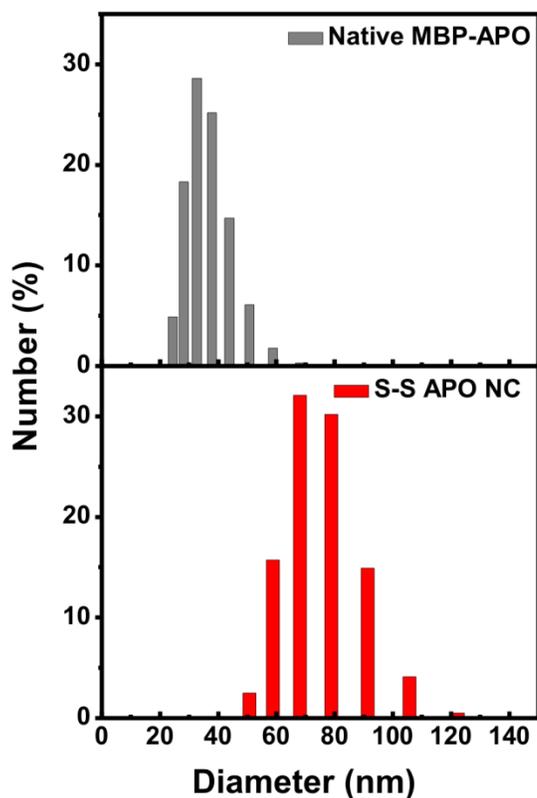

Supplement 3. Size distribution of native MBP-APO and S-S APO NC formed. The hydrodynamic sizes of the native MBP-APO (grey) and S-S APO NC (red) were determined by DLS.

S-S Rho-APO NC **ND Rho-APO NC**
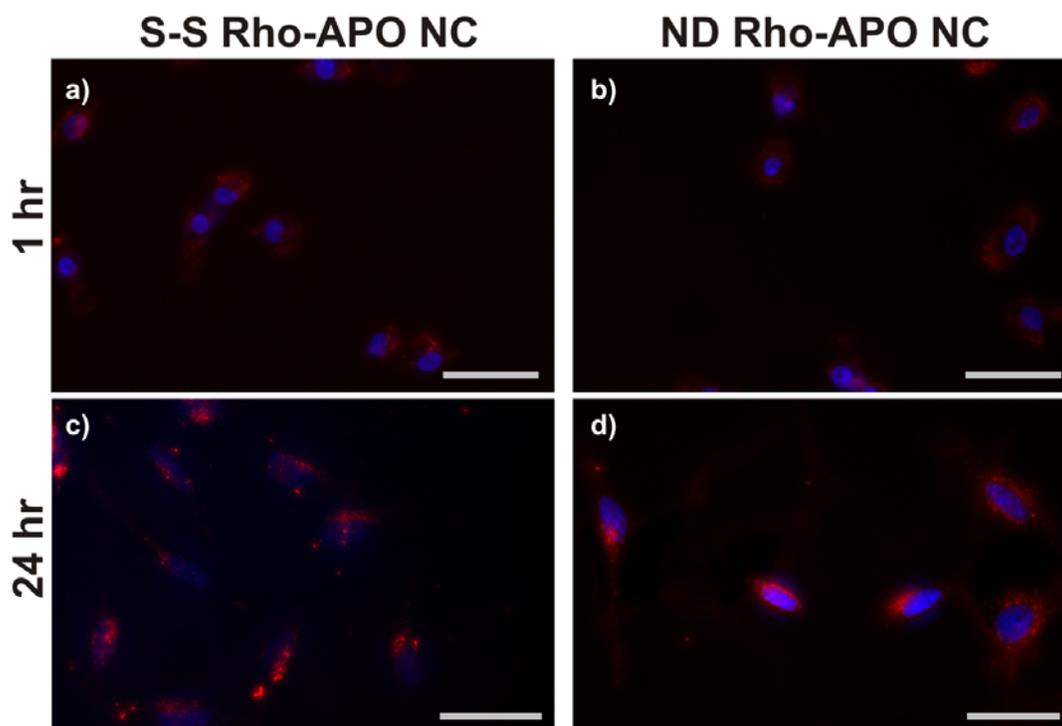
Supplement 4. Internalization of S-S APO NC and ND APO NC. Fluorescent microscope images of MDA-MB-231 cells after 1 and 24 hours incubation with 20 nM S-S Rho-APO NCs and with 20 nM ND Rho-APO NCs. Nuclei were stained with DAPI. The scale bars represent 50 μm.
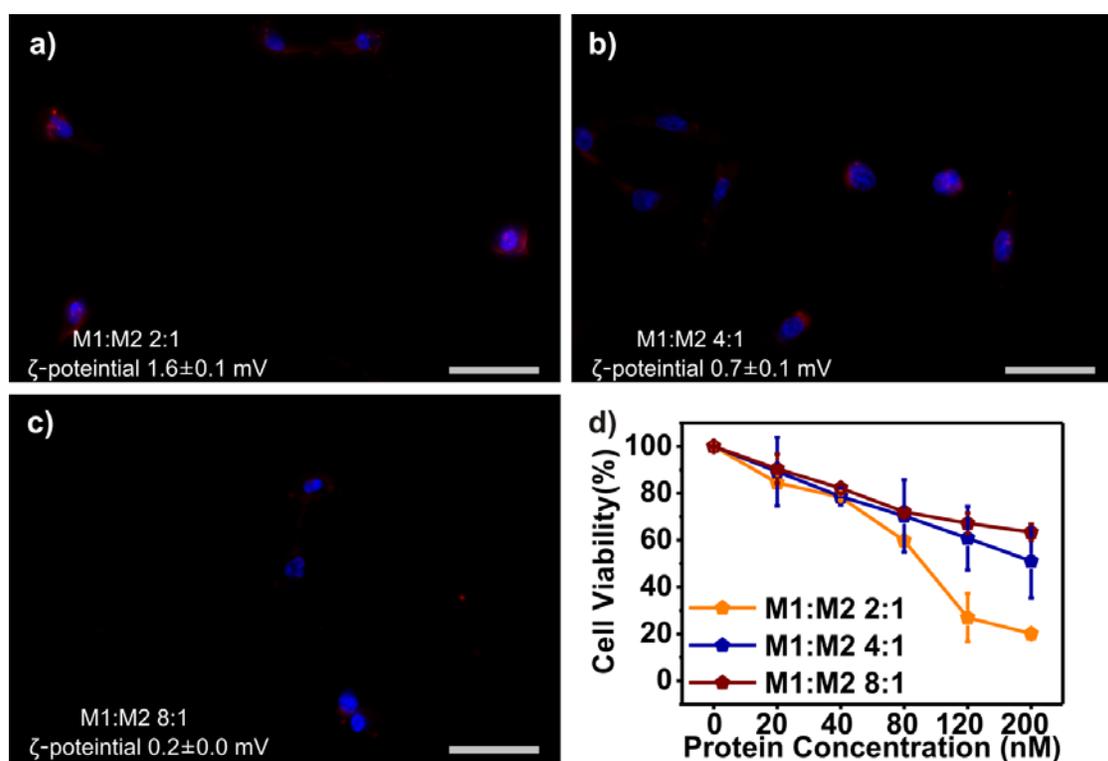
Supplement 5. Internalization and cytotoxicity of S-S APO NCs with different ζ-potentials. Fluorescent microscope images of MDA-MB-231 cells after 2 hours incubation with 20 nM S-S NCs of different M1 to M2 ratios a) 2:1; b) 4:1; and c) 8:1. Nuclei were stained with DAPI. The scale bars represent 50 μm; d) Cell viability curves for MDA-MB-231 cells treated with various concentrations of S-S APO NC with diffrent ζ-potentials.
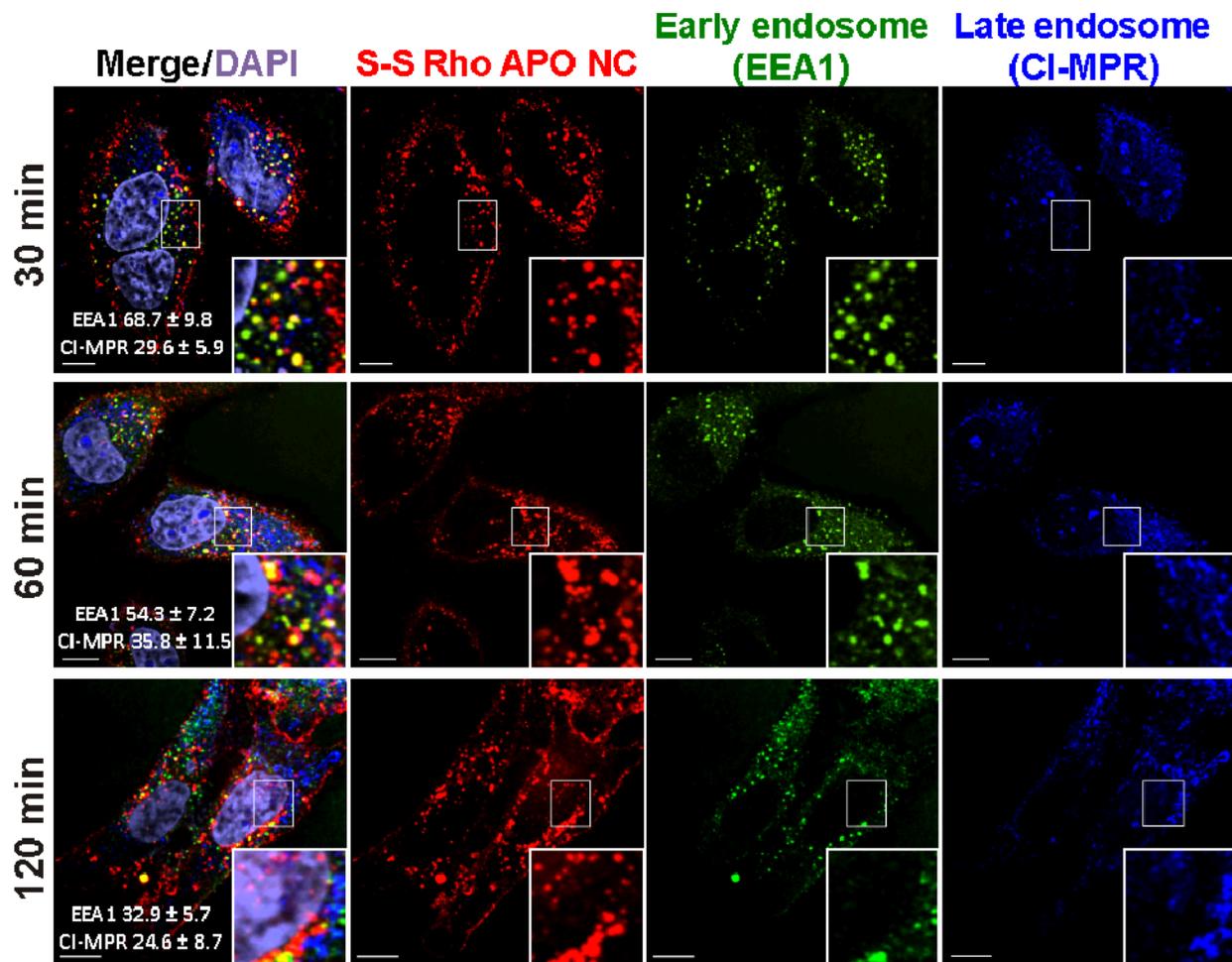
Supplement 6. S-S APO NC cellular trafficking shown with merged and indivisual channels. The trafficking of Rho-APO in S-S NCs through early and late endosomes. HeLa cells were incubated with 20 nM S-S Rho-APO NCs (red) at 37 °C for various time periods, 30, 60 and 120 min. Early endosomes were detected by early endosome antigen 1 (EEA1, green). Late endosomes were detected by cation-independent mannose-6-phosphate receptor (CI-MPR, blue). Nuclei were stained with DAPI and shown as purple. The scale bar represents 10 μm. The percentage of fluorescence colocalization was quantified by calculating colocalization coefficients using Manders' overlap coefficient (>10 samples) and shown in each figure.
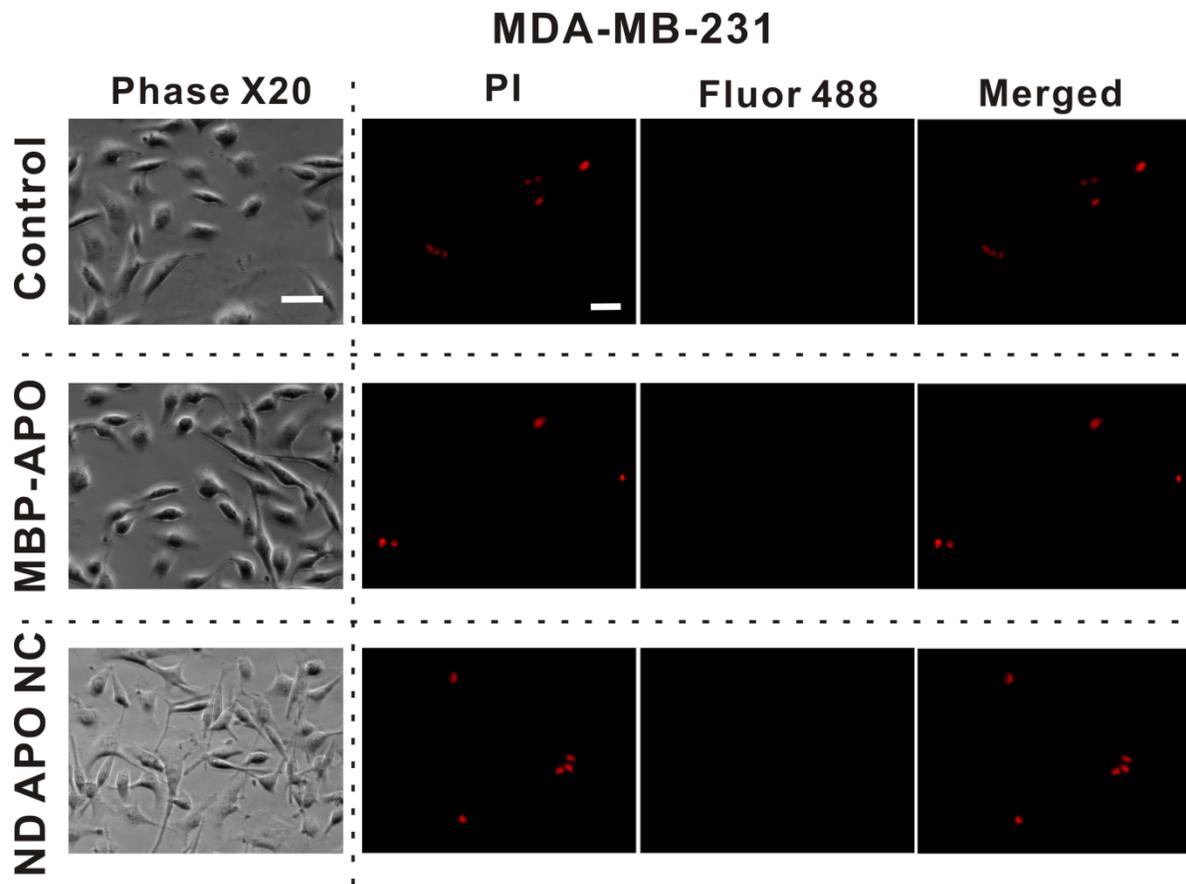
MDA-MB-231

Supplement 7. MDA-MB-231 cells TUNEL assay control groups. Left images of dash line are Bright-field-microscopy images of MDA-MB-231 treated for 24 hours with (i) control (saline); (ii) 200 nM native MBP APO; (iii) 200 nM ND APO NC. The scale bars represent 50 µm; Imagines right of dash line are apoptotic fragmentation of the nucleosome detected by APO-BrdU^{TM} TUNEL after same treatment as above. The scale bars represent 50 µm. Red fluorescence represents the PI-stained total DNA, and green Alexa Fluor 488 fluorescence represents apoptotic DNA fragmentation. The merged pictures combine the PI-stained nuclei and the Alexa Fluor 488-stained nick end label. Note the bright field images do not overlap with the fluorescent images.

Supplement 8 Additional experimental section

8.1 Instruments

The Bradford protein assay was carried out on a Thermo Scientific GENESYS 20 spectrometer. The size distribution and ζ-potential of NCs were measured on the Malvern particle sizer Nano-ZS. Transmission electron microscopy (TEM) images were obtained using Philips EM-120 TEM instrument. Fluorescent images were taken with Zeiss Axio Observer Z1 Inverted Microscope and Yokogawa spinning-disk confocal microscope (Solamere Technology Group, Salt Lake City, UT) on Nikon eclipse Ti-E Microscope equipped with a 60×1.49 Apo TIRF oil objective and a Cascade II: 512 EMCCD camera (Photometrics). An AOTF (acousto-optical tunable filter) controlled laser-merge system (Solamere Technology Group Inc.) was used to provide illumination power at each of the following laser lines: 491 nm, 561 nm, and 640 nm solid state lasers (50 mW for each laser).

8.2 Protein Expression and Purification method

The pMalTBVp3 plasmid for expression of the MBP-APO was a generous gift from Dr. C. Backendorf and Dr. M. Noteborn (Leiden University). MBP-APO plasmid was transformed into *Escherichia coli* BL21(DE3) cells and incubated at 37 °C overnight on LB agar plate with 100 μg/mL ampicillin. Colonies were picked and grown overnight at 37 °C with shaking (250 rpm) in 5 mL ampicillin-containing LB media. Overnight cultures were then inoculated in 500 mL of TB media with 100 μg/mL ampicillin and allowed to grow under 37 °C until the absorbance of cell density (OD_{600}) reached 1.0. Isopropyl *β*-D-1-thiogalactopyranoside (IPTG) was added to a final concentration of 0.1 mM to induce protein expression. After overnight incubation at 16 °C, cells were harvested by centrifugation (2,000 g, 4 °C, 15 min). MBP-APO protein was purified according to procedure described in previous literature (S. R. Leliveld, Y. H. Zhang, J. L. Rohn, M. H. Noteborn, J. P. Abrahams, *J Biol. Chem*. 278 (2003) 9042). Cell pellets were first resuspended in 30 mL lysis buffer (25 mM Tris-HCl, 500 mM NaCl, 10% glycerol pH 7.4) and lysed by sonication. Cell debris and insoluble proteins were removed by centrifugation (17,000 rpm, 4 °C, 30 min), followed by filtering through 0.22 μm filters to clear the cell lysate further. Protein was then purified on an amylase column (New England BioLabs), which was passed over 5 times with lysate under gravity flow at 4 °C then washed with wash buffer (20 mM Tris-HCL, 50mM NaCl, 1 mM EDTA, pH 7.4) to remove unbounded protein. MBP-APO was eluted from the column with 10 mM maltose buffer and buffer exchanged into PBS. The protein concentration was qualitatively assessed by SDS-PAGE and quantitatively determined by the Bradford protein assay using bovine serum albumin (BSA) as the standard.